NASA TM X-364

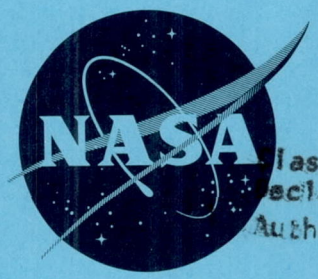

TECHNICAL MEMORANDUM
X-364

THE EFFECTS OF WING PLAN FORM ON THE STATIC LONGITUDINAL AERODYNAMIC CHARACTERISTICS OF A FLAT-TOP HYPERSONIC AIRCRAFT AT MACH NUMBERS FROM 0.6 TO 1.4

By Stuart L. Treon

Ames Research Center
Moffett Field, Calif.

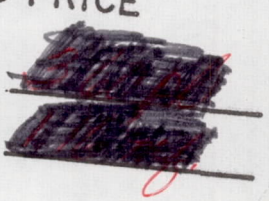

NATIONAL AERONAUTICS AND SPACE ADMINISTRATION
WASHINGTON
April 1960

NATIONAL AERONAUTICS AND SPACE ADMINISTRATION

TECHNICAL MEMORANDUM X-364

THE EFFECTS OF WING PLAN FORM ON THE STATIC LONGITUDINAL AERODYNAMIC CHARACTERISITICS OF A FLAT-TOP HYPERSONIC AIRCRAFT AT MACH NUMBERS FROM 0.6 TO 1.4*

By Stuart L. Treon

SUMMARY

A wind-tunnel investigation at Mach numbers of 0.6 to 1.4 has been conducted to determine some effects of wing plan form on the static longitudinal aerodynamic characteristics of a hypersonic aircraft configuration. The configurations tested consisted of three arrow-plan-form wings mounted atop a slender half-cone body. The angle of attack ranged from -7° to $+23^{\circ}$. Test Reynolds number was 1.75 million or 2.5 million referred to the model body length.

For the three wings investigated, there were no significant effects on the aerodynamic characteristics of the flat-top configuration due to changes in plan form. The lift-curve slope at sonic speed was closely estimated for two of the models by means of slender-wing theory, ignoring possible wing-body interference. Values of maximum lift-drag ratio and locations of the stick-fixed neutral point at Mach number 1.4 were in close agreement with those obtained for similar models at Mach number 3.0 in a previous investigation.

INTRODUCTION

Interest in aircraft capable of efficient flight at high supersonic speeds has led to proposals of several configurations, some of which are discussed in references 1 through 4. One proposed configuration is designed to obtain high lift-drag ratios by utilizing favorable aerodynamic interference between the fuselage and the wing. The configuration consists of a thin, low-aspect-ratio wing of arrow plan form affixed to the upper surface of a body composed of the lower half of a right circular cone. The resulting shape is characterized by an upper surface which is nearly plane.

*Title, Unclassified

Tests of several such "flat top" models, conducted at Mach numbers from 3.0 to 6.28 (ref. 1), indicated promising values of maximum lift-drag ratio. These tests were supplemented with wind-tunnel investigations of additional configurations at Mach numbers of 3.0 to 6.28 (ref. 5) and investigations of the low-speed and landing characteristics of some of these flat-top models (ref. 6). The results of a study of the performance and stability and control characteristics of several such configurations at Mach numbers from 0.6 to 18 are reported in reference 7.

Although the high-speed characteristics of flat-top configurations have been somewhat extensively investigated as evidenced in the foregoing references, relatively little is known of the transonic characteristics of such shapes. The purpose of this report is to present the transonic static longitudinal characteristics of three flat-top models having different wing plan forms.

NOTATION

AR	aspect ratio, $\frac{b^2}{S}$
b	wing span
c	wing chord
C_D	forebody drag coefficient, $\frac{\text{drag}}{qS}$
$C_{D_{min}}$	minimum forebody drag coefficient
C_L	lift coefficient, $\frac{\text{lift}}{qS}$
C_{L_α}	lift-curve slope, per deg
$C_{L_{opt}}$	lift coefficient for maximum lift-drag ratio
C_m	pitching-moment coefficient, $\frac{\text{pitching moment about center of body volume}}{qSl}$
$C_{m_{C_L}}$	pitching-moment-curve slope
$\left(\frac{L}{D}\right)_{max}$	maximum lift-drag ratio
l	length of body
M	Mach number

q	free-stream dynamic pressure
R	Reynolds number
S	wing plan-form area including area over body (See fig. 1 for values.)
t	wing thickness
α	angle of attack, deg

APPARATUS AND MODELS

The investigation was made in the Ames 2-Foot Transonic Wind Tunnel, which is described in reference 8. The principal feature of the tunnel is a perforated test section which permits continuous, choke-free operation from subsonic speeds up to Mach number 1.4.

Three models were tested (see fig. 1). All three were similar to configurations previously tested at low speeds (ref. 6) and at Mach numbers above 3 (refs. 1, 5, and 7). As may be seen in the figure, each model consists of a body formed from the lower half of a right circular cone on the plane surface of which is affixed a thin arrow-plan-form wing having the leading edges swept back 77.4°. Model A is the basic model; model A_{45} and model B are variations that resulted from altering the rear portion of the wing for model A. Model A_{45} was obtained from model A by bending the outer portion of the wing 45° downward, resulting in drooped tips equal to 18.25 percent of the unbent plan area (the drooped tips possibly providing a means of directional stability and control). Model B was obtained by extending the trailing edge (the added wing area possibly providing a means of pitch and roll control as well as a more rearward neutral point location for increased static stability).

Lift and drag forces were measured with a strain-gage balance positioned behind the model as shown in figure 2. The model was attached to the balance by a sting. Pitching moments were measured with a strain gage fastened to the sting. The sting and the balance were encased in a shroud which extended to within about 0.03 inch of the base of the body.

To obtain the range of angles of attack required in this investigation (-7° to +23°) it was necessary to amplify the travel normally provided by the angle-of-attack mechanism. This was accomplished by the use of two stings, one straight and one bent. With either sting the model was pitched about a point on the center line of the tunnel approximately 1 inch forward of the model base.

TESTS AND DATA REDUCTION

Lift, drag, and pitching moment were measured for all models at angles of attack from approximately -7° to $+23^\circ$ at ten Mach numbers from 0.6 to 1.4. Below 8° angle of attack the Reynolds number of the tests (based upon the length of the body, i.e., 7.14 in.) was 2.5 million, and from 8° to 23° it was 1.75 million. The reduction of Reynolds numbers at the higher angles of attack was necessary to prevent overloading of the balance.

The models were equipped with trip wires to ensure turbulent flow in the boundary layer. The trip wires were approximately 0.004 inch in diameter and were located on the upper and lower surfaces of the models, as shown in figure 1. The data of references 9 and 10 were used to choose this wire size. In order to determine the effectiveness of the trip wire, the forebody drag coefficient at $M = 0.6$ for model A was calculated assuming a turbulent boundary layer. In making the calculation it was further assumed that for such a slender shape there would be no pressure drag at $M = 0.6$, and that all drag would result from skin friction. The value used for the skin-friction coefficient was obtained from reference 11. It was found that the calculated value agreed very well with the corresponding experimental result, 0.0086 vs. 0.0082, thus indicating that at least at $M = 0.6$ the wires effectively tripped the boundary layer as desired.

No corrections have been applied to the data for wall interference. At subsonic Mach numbers the magnitude of such corrections, estimated according to the method of reference 12, was found to be negligibly small. At transonic and supersonic Mach numbers, although no information is available for determining the corrections to be applied to data for wing-body models with highly sweptback wings, information is available for models with unswept wings (ref. 13). This information indicates that, even for models larger relative to the wind-tunnel test section than those of the present investigation, the wall interference is insignificant. It is therefore concluded for the present investigation that wall interference throughout the range of test Mach numbers was negligible.

The forebody drag coefficients were obtained by adjusting the measured drag forces to account for the difference between the actual pressure at the base of the model, measured in the presence of the sting, and an assumed condition of free-stream static pressure acting across the base of the model.

The method of reference 14 was used to analyze the precision of the data of this report and the average deviations of values of the data were determined to be approximately as follows:

M	±0.003
α	±0.05°
C_D	±0.001
C_L	±0.001
C_m	±0.002

RESULTS AND DISCUSSION

Basic aerodynamic characteristics of the models are presented in figures 3 through 11. The effects of wing plan form on the variations with Mach number of the lift-curve and pitching-moment-curve slopes are shown for three lift coefficients in figures 12 and 13, respectively. Additional summary plots of maximum lift-drag ratio, optimum lift coefficient, and minimum drag coefficient as functions of Mach number are presented in figure 14.

At positive lift coefficients, the basic pitching-moment curves particularly, and to a lesser extent the basic lift curves, were characterized essentially by two straight lines, the intersections of which occurred at lift coefficients of about 0.08 for model A, 0.25 for model A_{45}, and 0.20 for model B (figs. 3 through 8). Otherwise, the variations of the data were smooth and regular throughout the angle-of-attack range as might be expected for such slender configurations.

The effect of wing plan form on the lift-curve slope was of no great significance (fig. 12) - the values being low but of the order associated with such slender plan forms. It is interesting to note that for a triangular wing alone having the same sweep and span as configurations A and B, the lift-curve slope at sonic speed according to slender-wing theory is 0.0245 per degree. This value compares favorably with the experimental values at $M = 1.0$ of 0.0240 and 0.234 for configurations A and B, respectively. Such an estimate, of course, neglects any possible aerodynamic interference between the wing and the body.

Evident in the basic curves of figures 6, 7, and 8 is a decrease in stability at lift coefficients above that for maximum lift-drag ratio. A similar result was observed in the low-speed data of reference 6. The over-all variation of pitching-moment-curve slope with Mach number is indicative of increasing stability with increasing Mach number and is much the same for the three models. Throughout the Mach number range, the locations of the stick-fixed neutral points (equivalent to the values of the pitching-moment-curve slopes at $C_L = 0$, in figure 13, as adjusted to

the moment reference station at 0.75l) were within 0.05l of the respective centroids of wing plan area (0.75l for model A, 0.71l for model A_{45}, and 0.80l for model B). Of interest also was the fact that the stick-fixed neutral points for models A and B at M = 1.4 were essentially at the same locations as those reported in reference 1 for very similar configurations at M = 3.0.

There was no significant effect of wing plan form on maximum lift-drag ratio, lift coefficient for maximum lift-drag ratio, or minimum drag coefficient either in magnitude or in variation with Mach number, as can be seen in figure 14. The values of maximum lift-drag ratio for configurations A and B at M = 1.4 are essentially the same as those reported in reference 1 for similar configurations at M = 3.0.

CONCLUDING REMARKS

A wind-tunnel investigation of a flat-top hypersonic aircraft configuration at Mach numbers from 0.6 to 1.4 indicates that for three variations in arrow-wing plan form there were no significant effects on the longitudinal aerodynamic characteristics due to changes in plan form. A good estimate of the lift-curve slope at sonic speed was made for two of the models by means of slender-wing theory applied to a triangular wing of appropriate sweep and span, ignoring possible wing-body interference. Values of maximum lift-drag ratio and locations of the stick-fixed neutral point at Mach number 1.4 were in close agreement with those values obtained for similar models at Mach number 3.0 in a previous investigation.

Ames Research Center
National Aeronautics and Space Administration
Moffett Field, Calif., Dec. 31, 1959

REFERENCES

1. Eggers, A. J., Jr., and Syvertson, Clarence A.: Aircraft Configurations Developing High Lift-Drag Ratios at High Supersonic Speeds. NACA RM A55L05, 1956.

2. Seiff, Alvin, and Allen, H. Julian: Some Aspects of the Design of Hypersonic Boost-Glide Aircraft. NACA RM A55E26, 1955.

3. Ferri, Antonio, Clarke, Joseph H., and Casaccio, Anthony: Drag Reduction in Lifting Systems by Advantageous Use of Interference. PIBAL Rep. 272, Polytechnic Institute of Brooklyn, Dept. of Aeronautical Engineering and Applied Mechanics, May 1955.

4. Rossow, Vernon J.: A Theoretical Study of the Lifting Efficiency at Supersonic Speeds of Wings Utilizing Indirect Lift Induced by Vertical Surfaces. NACA RM A55L08, 1956.

5. Syvertson, Clarence A., Wong, Thomas J., and Gloria, Hermilo R.: Additional Experiments With Flat-Top Wing-Body Combinations at High Supersonic Speeds. NACA RM A56I11, 1957.

6. Kelly, Mark W.: Wind-Tunnel Investigation of the Low-Speed Aerodynamic Characteristics of a Hypersonic Glider Configuration. NACA RM A58F03, 1958.

7. Syvertson, Clarence A., Gloria, Hermilo R., and Sarabia, Michael F.: Aerodynamic Performance and Static Stability and Control of Flat-Top Hypersonic Gliders at Mach Numbers From 0.6 to 18. NACA RM A58G17, 1958.

8. Spiegel, Joseph M., and Lawrence, Leslie F.: A Description of the Ames 2- by 2-Foot Transonic Wind Tunnel and Preliminary Evaluation of Wall Interference. NACA RM A55I21, 1956.

9. Luther, Marvin: Fixing Boundary-Layer Transition on Supersonic-Wind-Tunnel Models (II). JPL Progress Rep. No. 20-287, Feb. 1956.

10. Winter, K. G., Scott-Wilson, J. B., and Davies, F. V.: Methods of Determination and of Fixing Boundary-Layer Transition on Wind Tunnel Models at Supersonic Speeds. A.R.C. C.P. No. 212, British, Sept. 1954. (Also available as AGARD Rep. AG 17/p7, Nov. 1954)

11. Locke, F. W. S., Jr.: Recommended Definition of Turbulent Friction in Incompressible Fluids. NAVAER DR Rep. No. 1415, June 1952.

12. Baldwin, Barrett S., Jr., Turner, John B., and Knechtel, Earl D.: Wall Interference in Wind Tunnels With Slotted and Porous Boundaries at Subsonic Speeds. NACA TN 3176, 1954.

13. Stivers, Louis S., Jr., and Lippmann, Garth W.: Effects of Fixing Boundary-Layer Transition for an Unswept-Wing Model and an Evaluation of Porous Tunnel-Wall Interference for Mach Numbers From 0.60 to 1.40. NACA TN 4228, 1958.

14. Beers, Yardly: Introduction to the Theory of Error. Addison-Wesley Publishing Co., Cambridge, Mass., 1953.

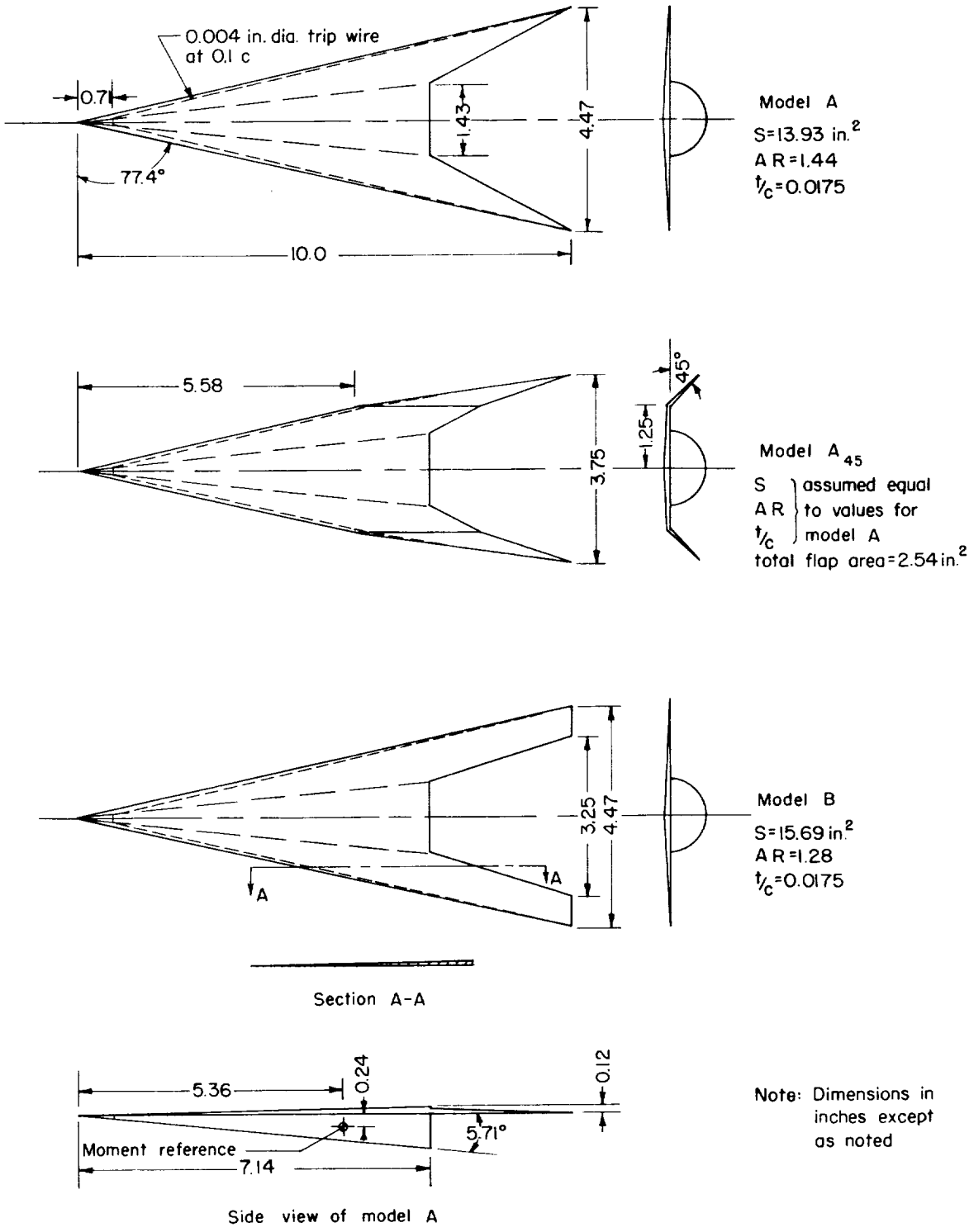

Figure 1.- Sketches and dimensions of models.

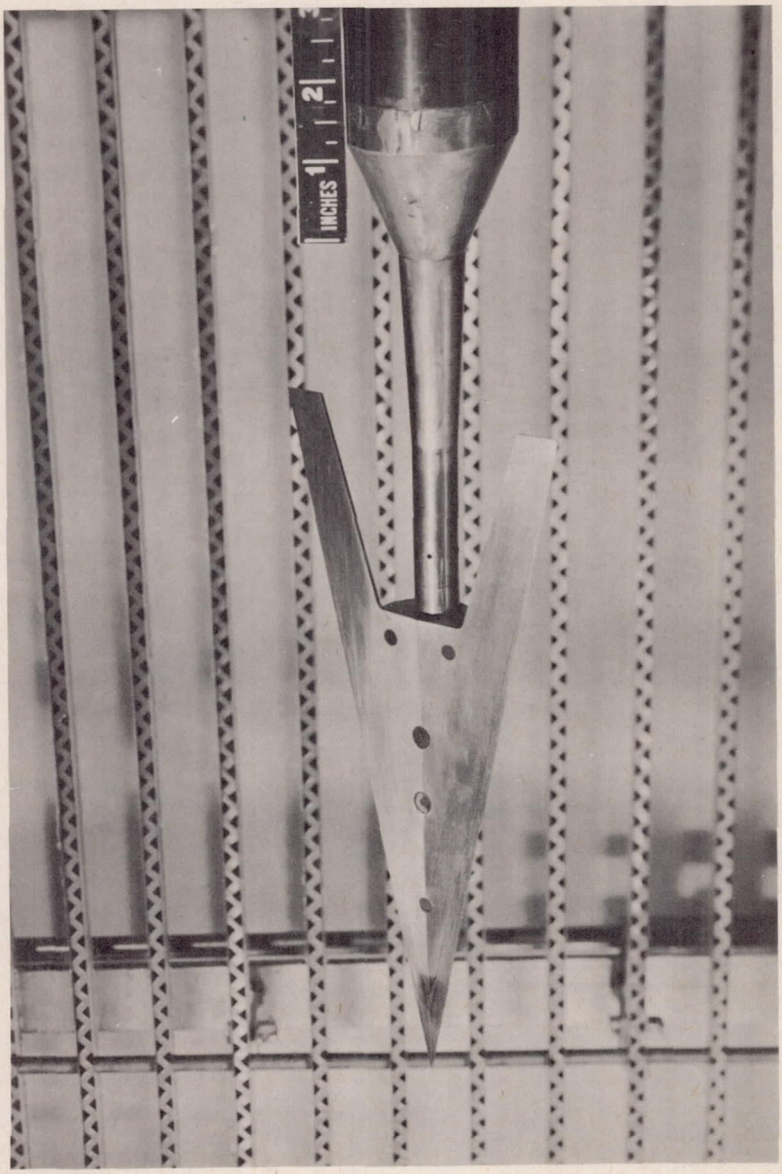

A-21754

Figure 2.- Typical model installed in test section.

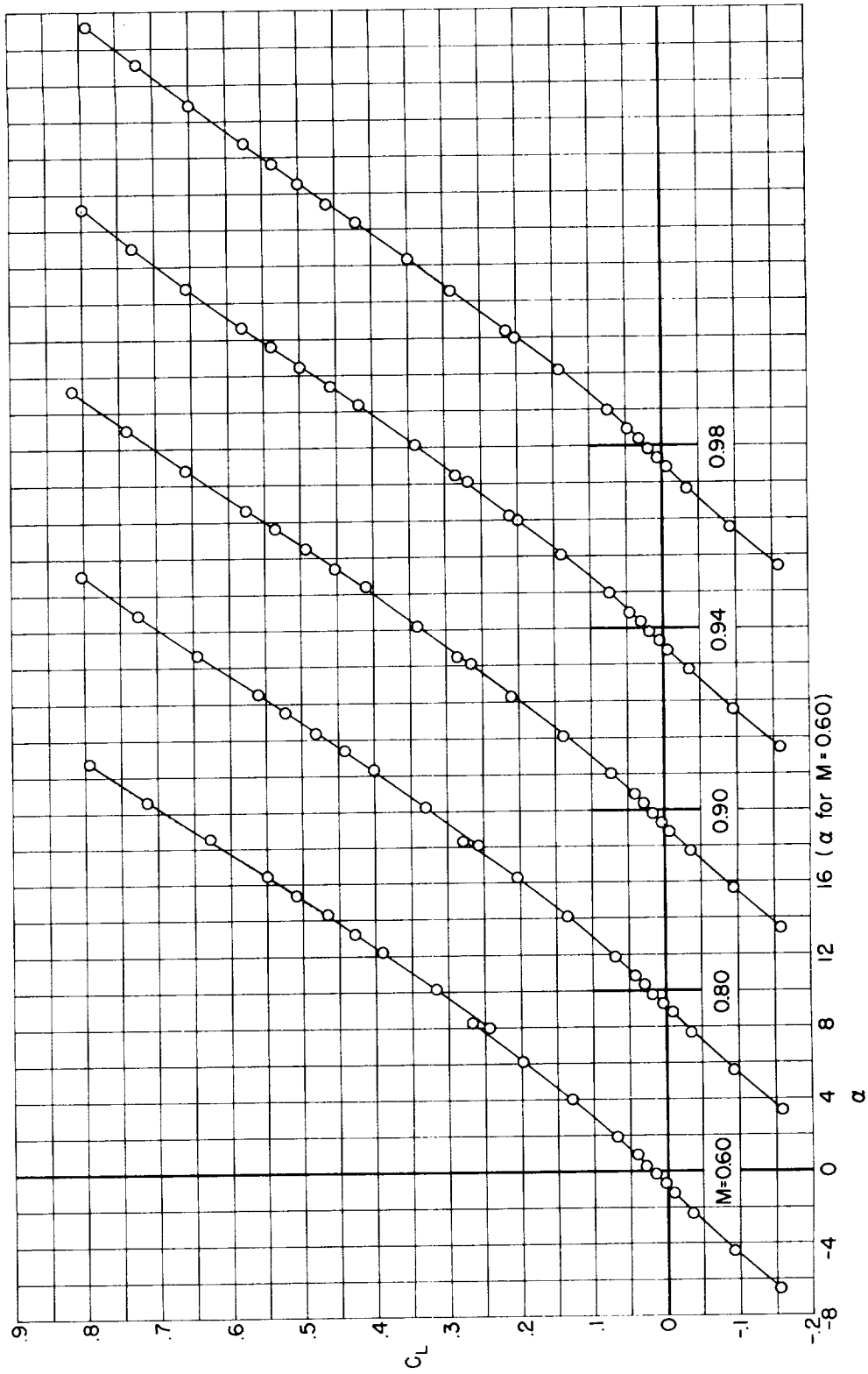

Figure 3.- Lift coefficient for model A.

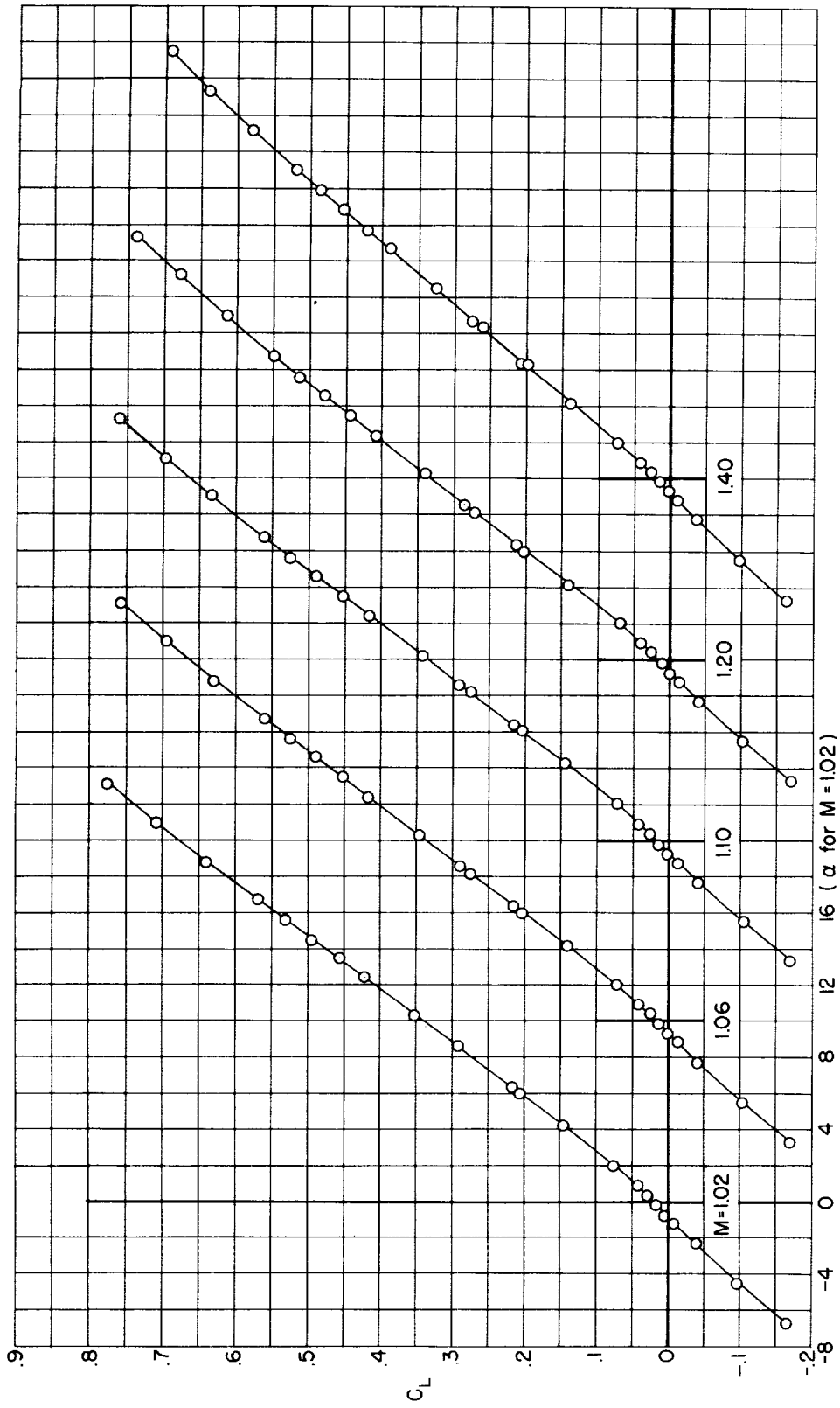

Figure 3.- Concluded.

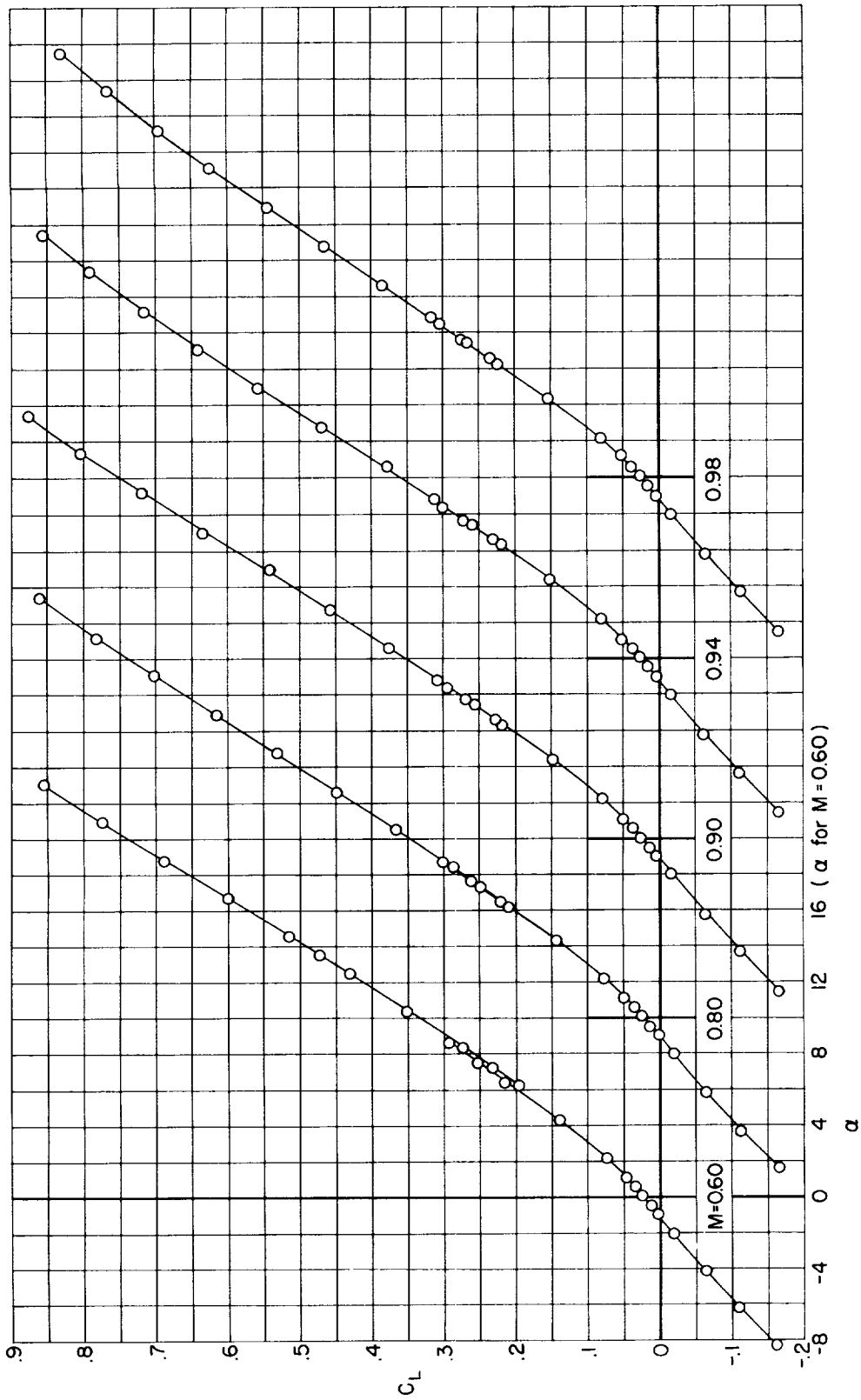

Figure 4.- Lift coefficient for model A_{45}.

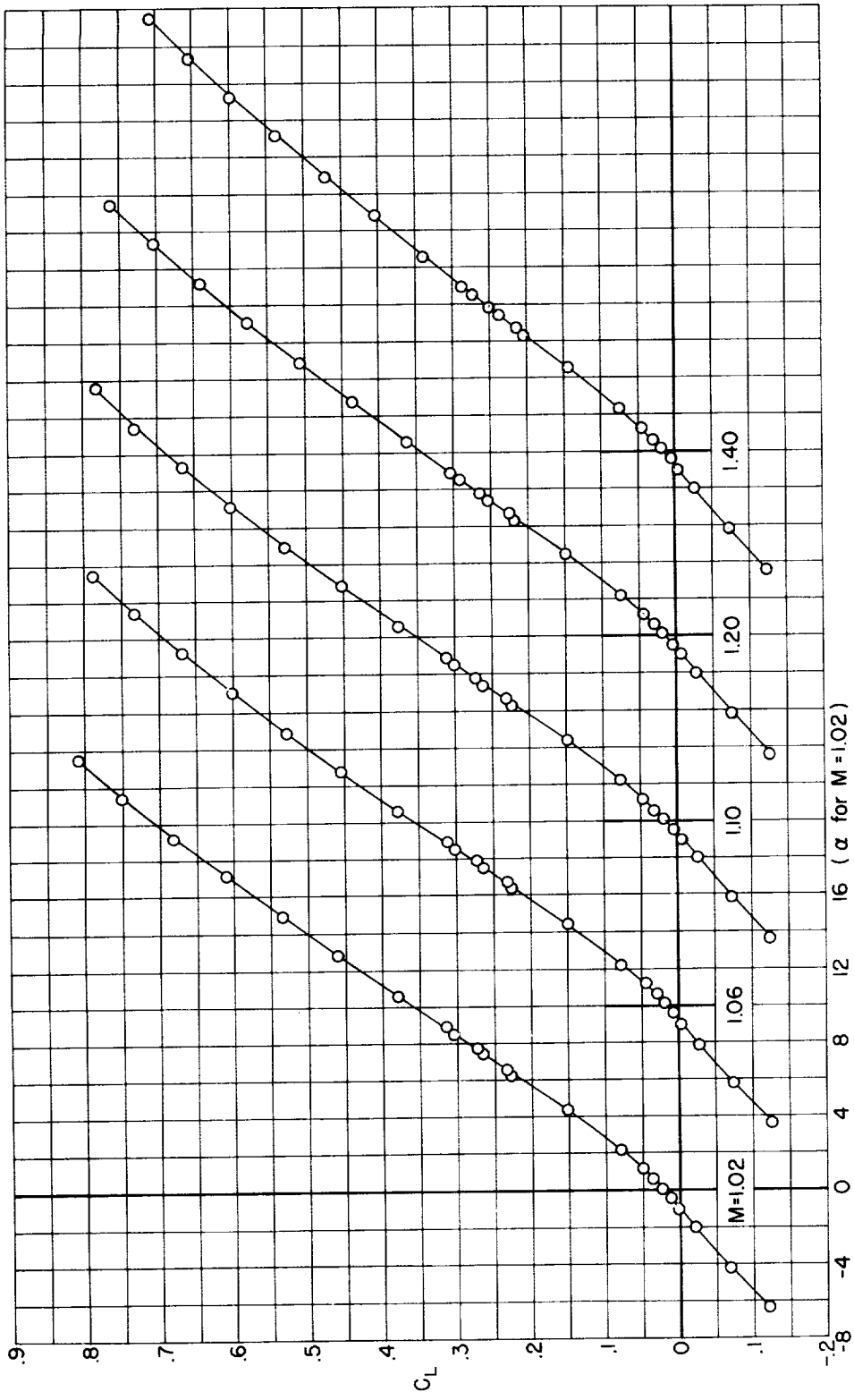

Figure 4.- Concluded.

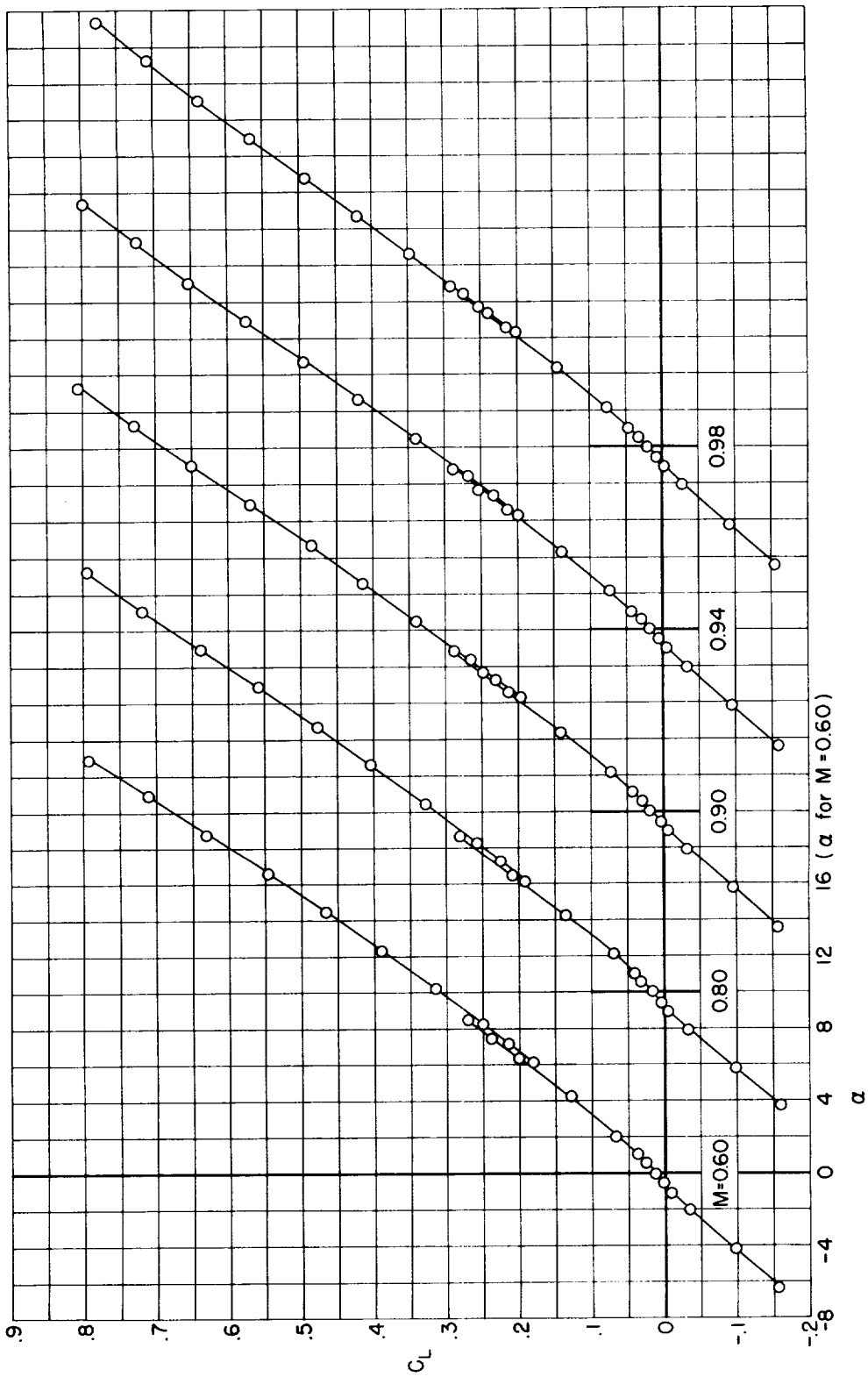

Figure 5.- Lift coefficient for model B.

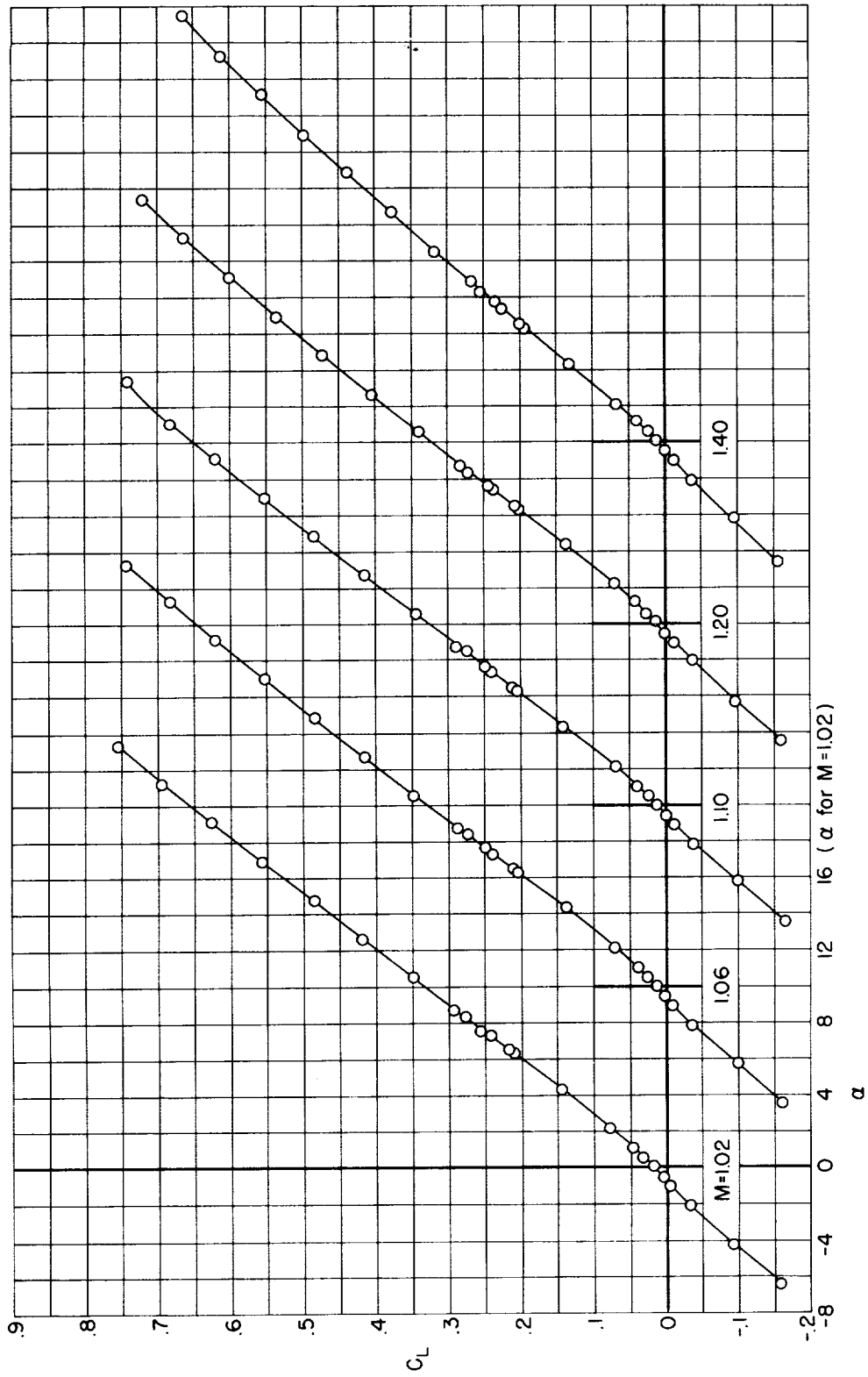

Figure 5.- Concluded.

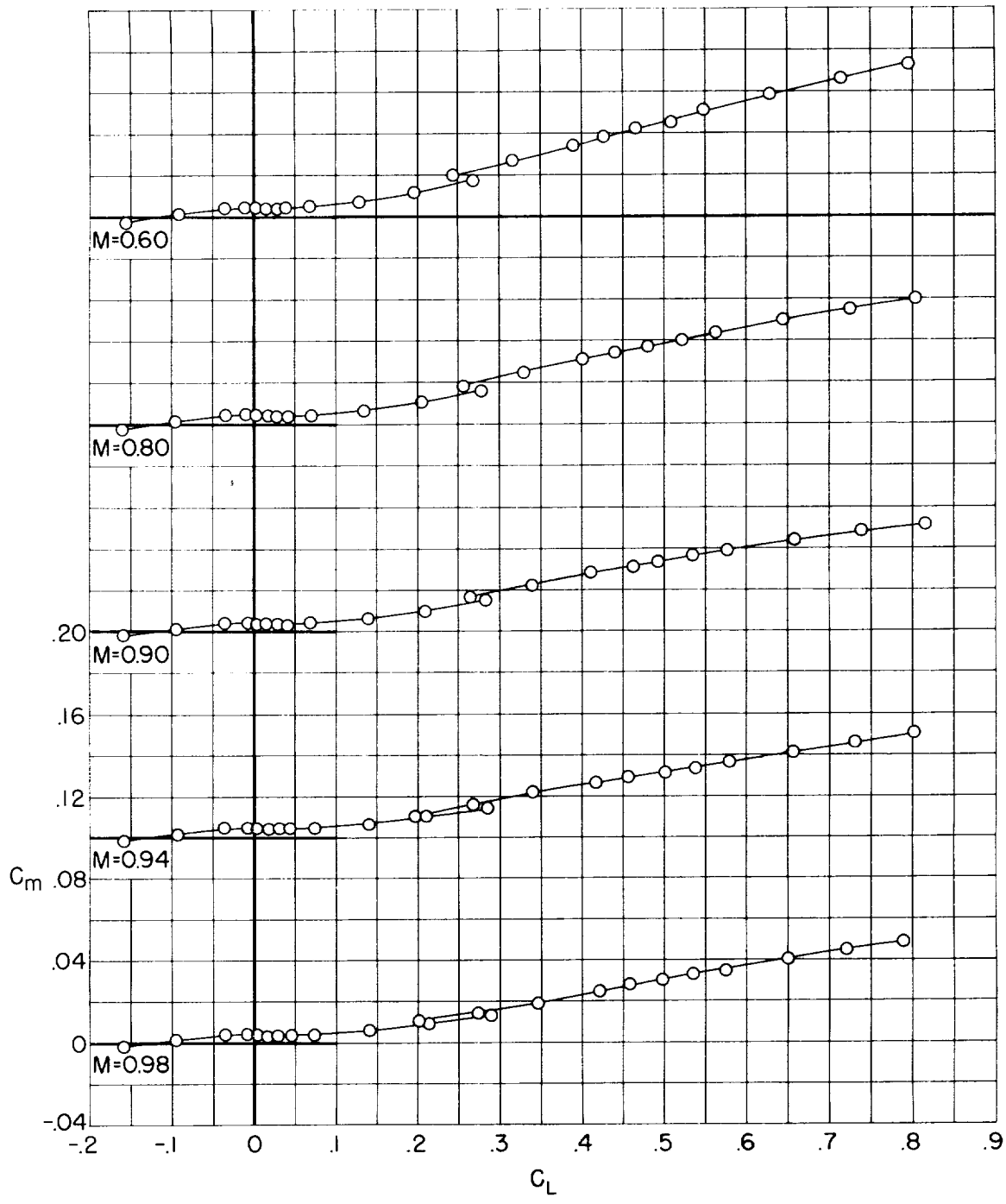

Figure 6.- Pitching-moment coefficient for model A.

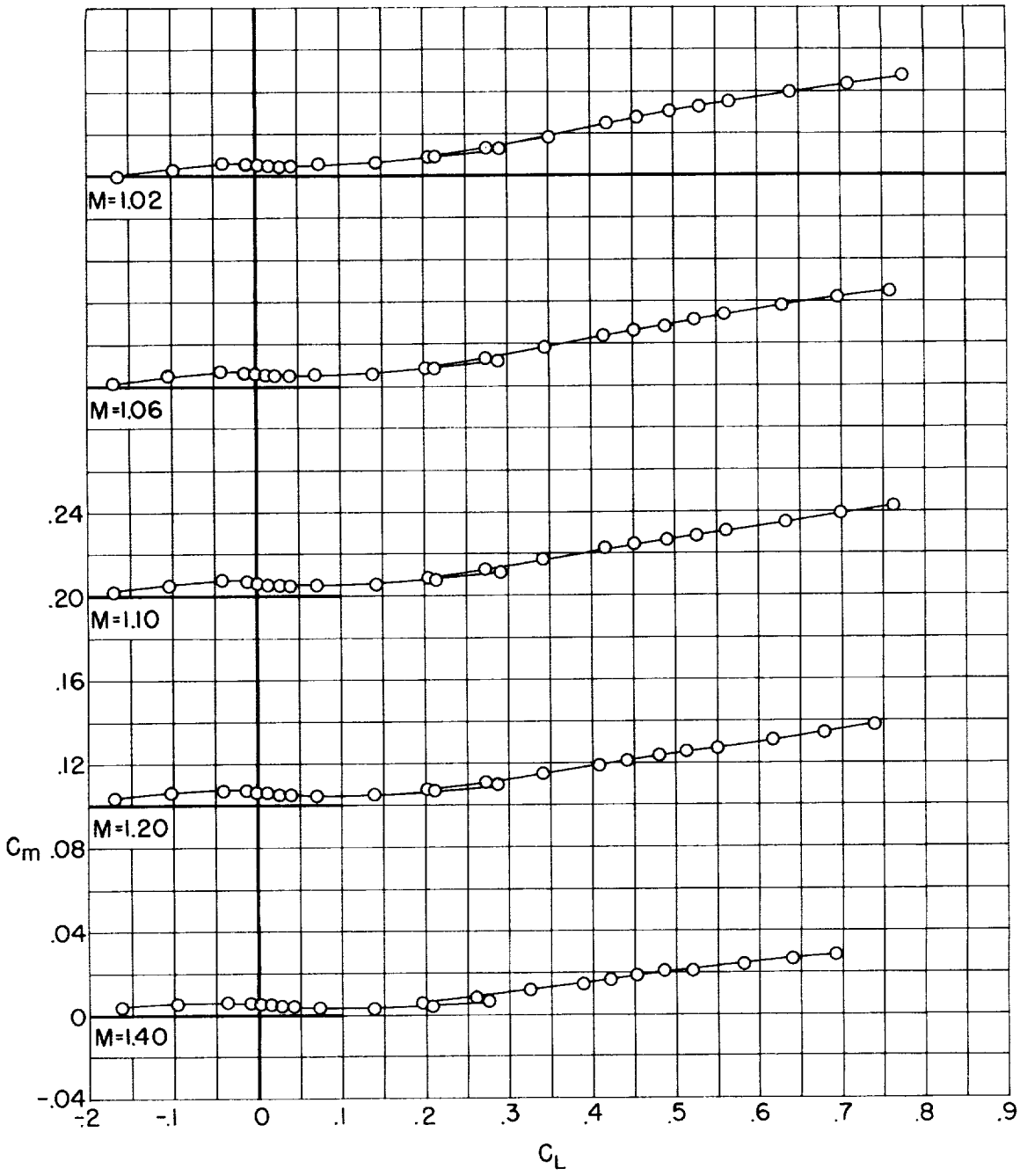

Figure 6.- Concluded.

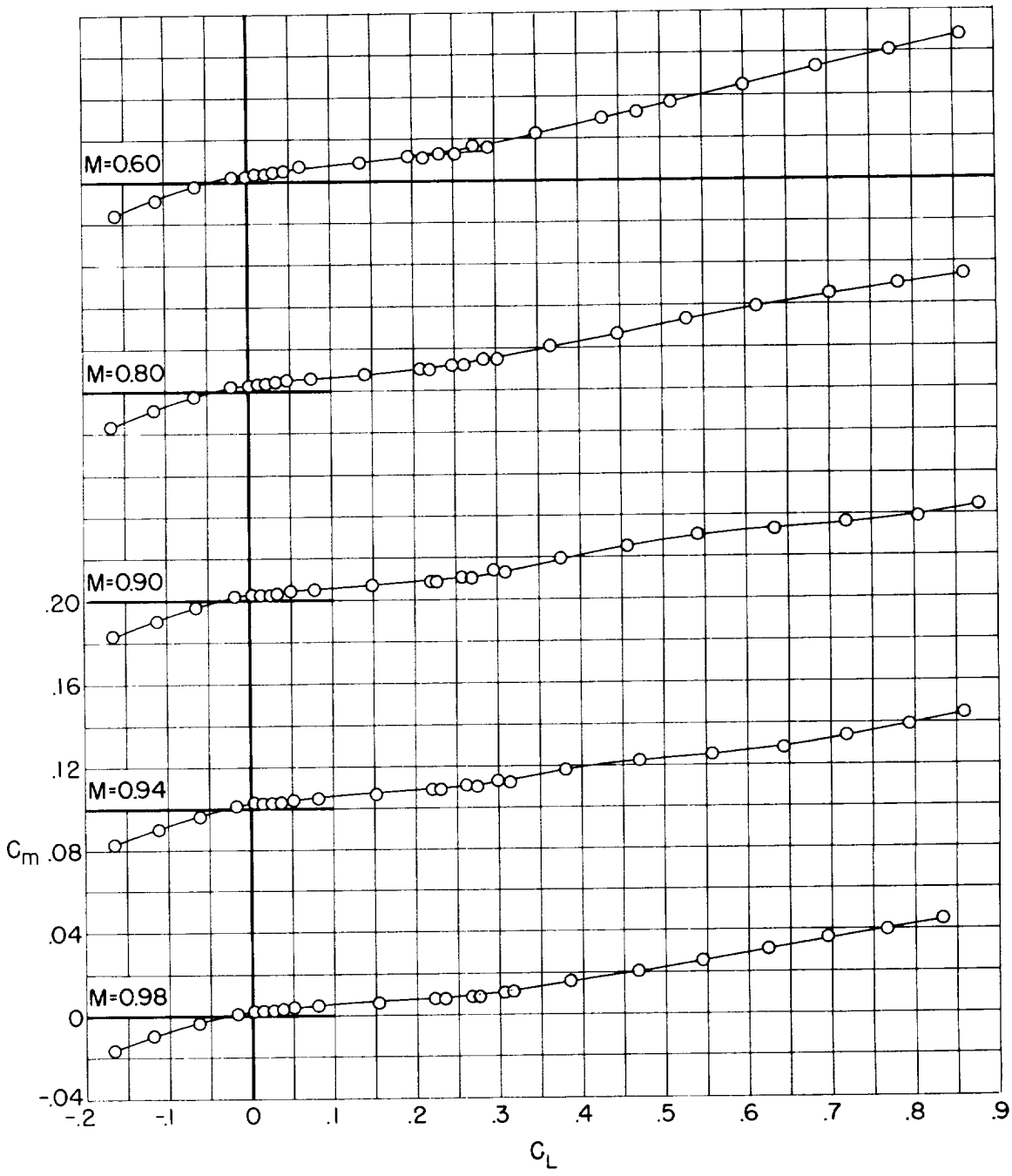

Figure 7.- Pitching-moment coefficient for model A_{45}.

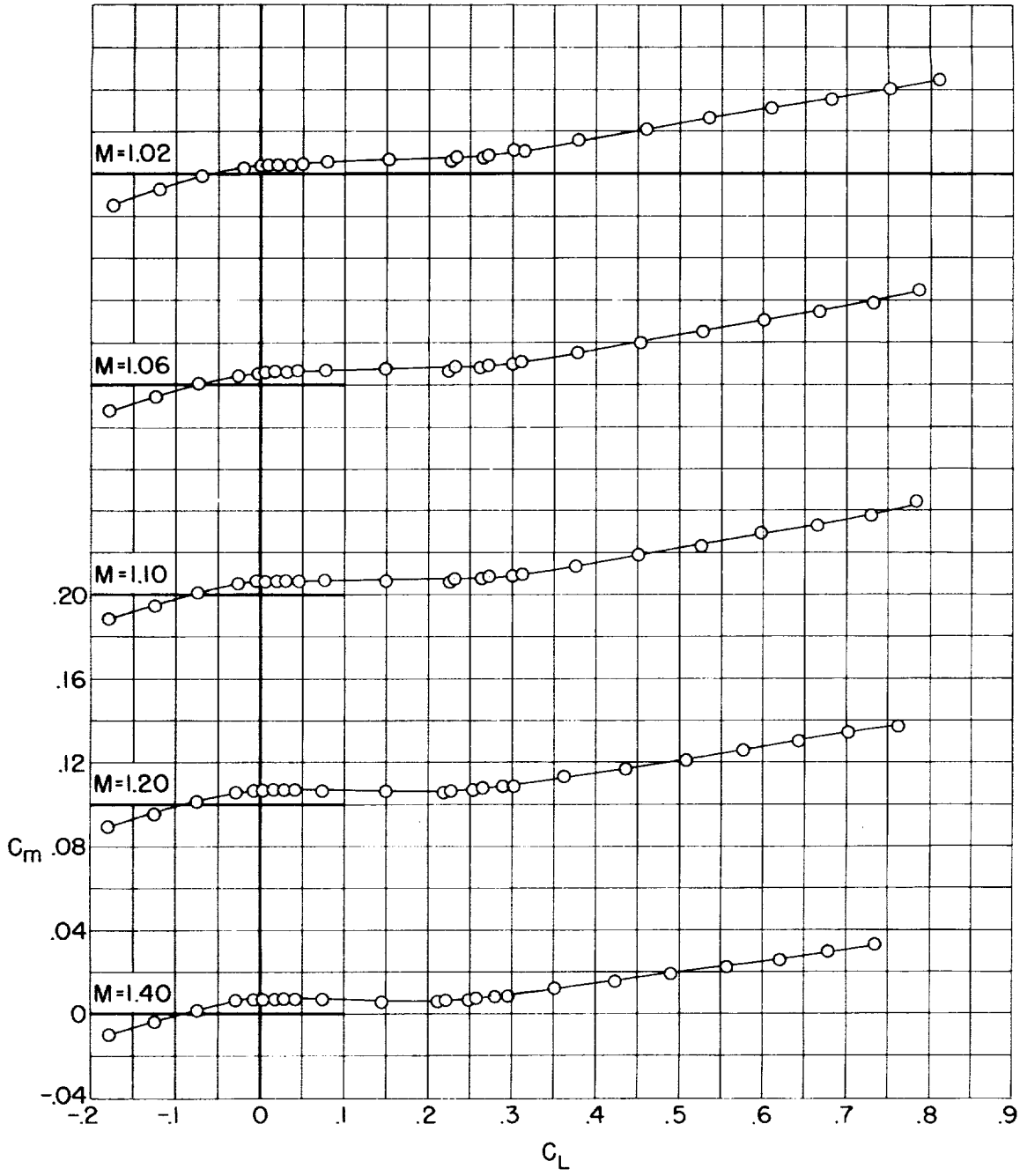

Figure 7.- Concluded.

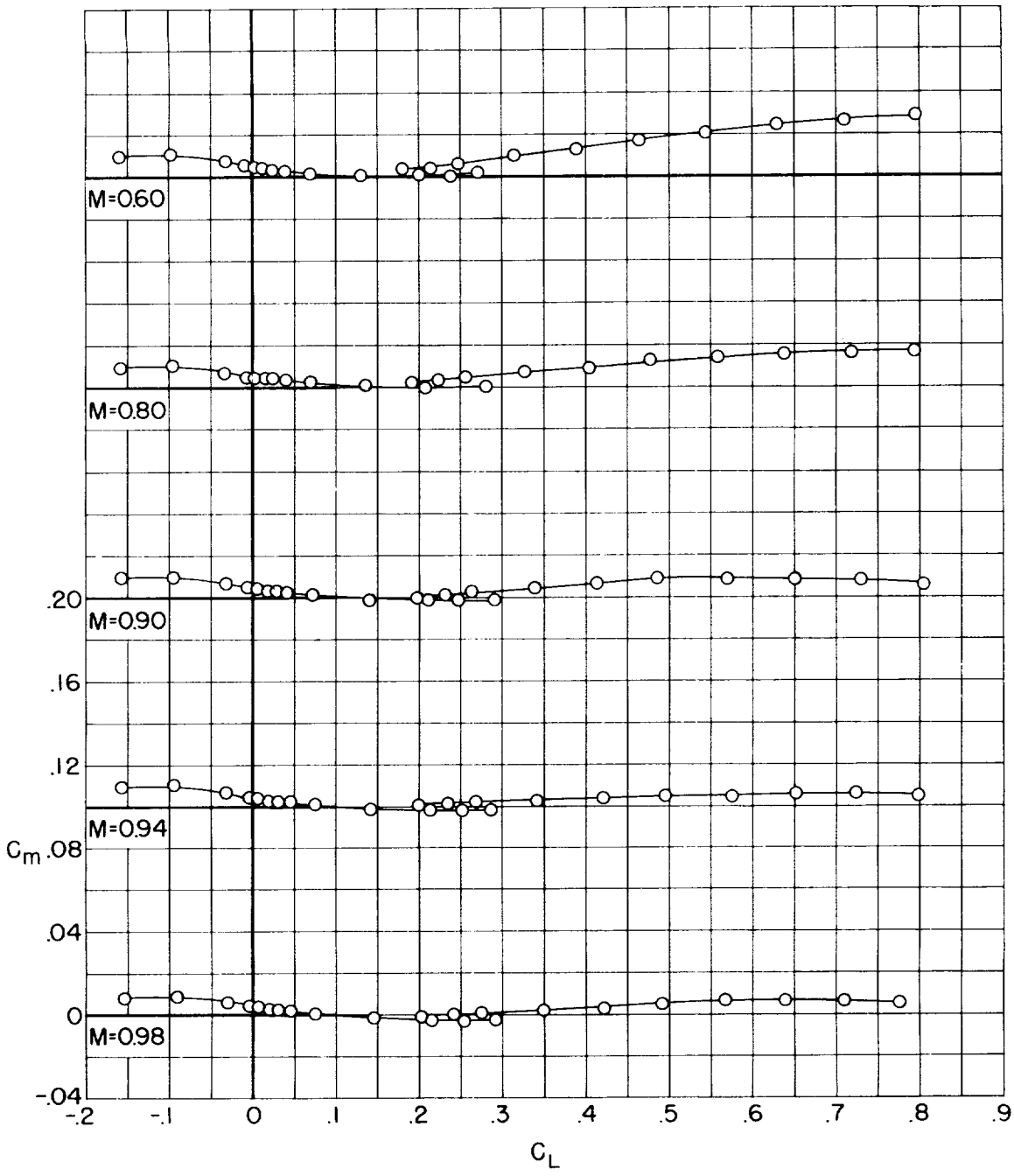

Figure 8.- Pitching-moment coefficient for model B.

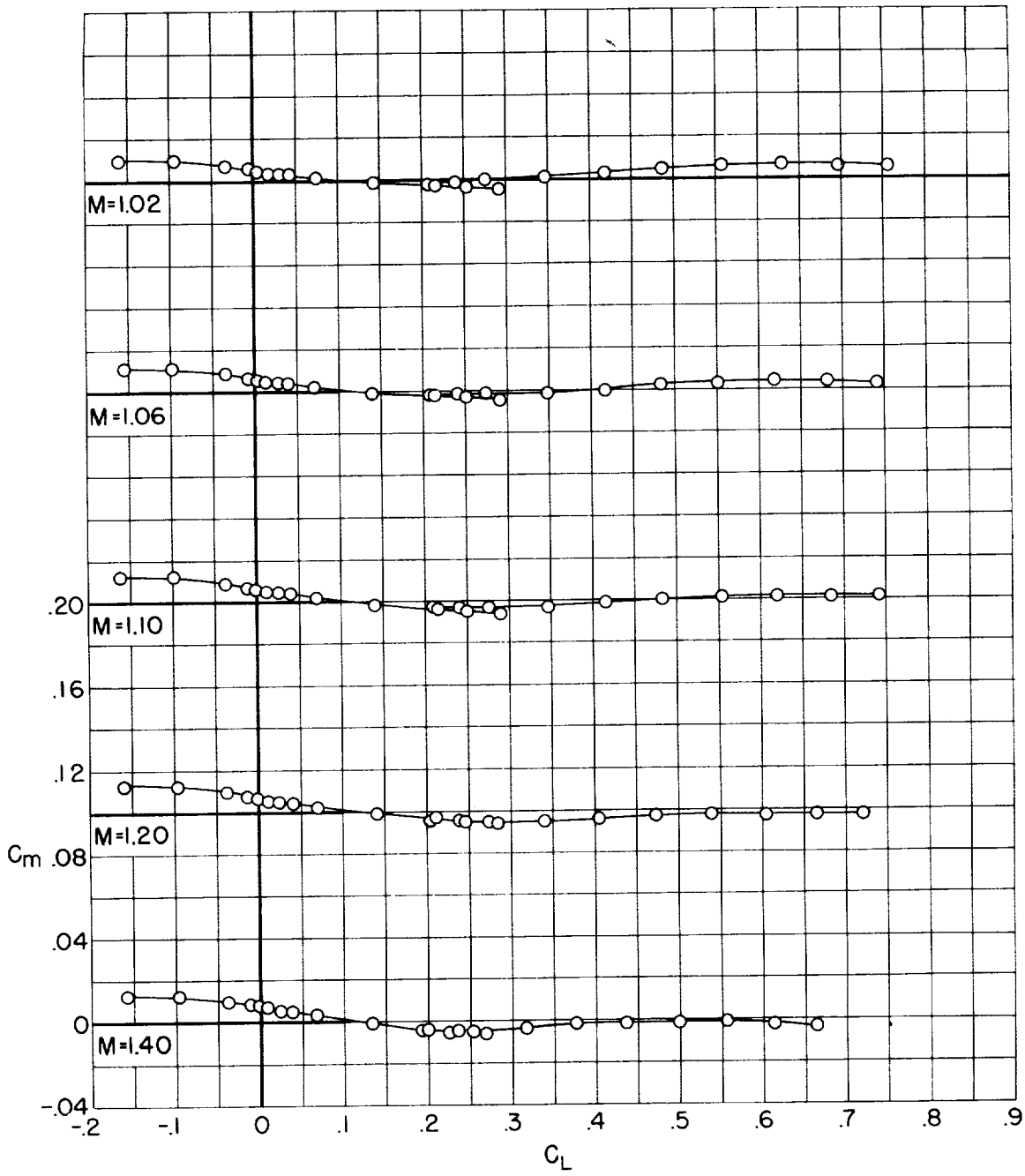

Figure 8.- Concluded.

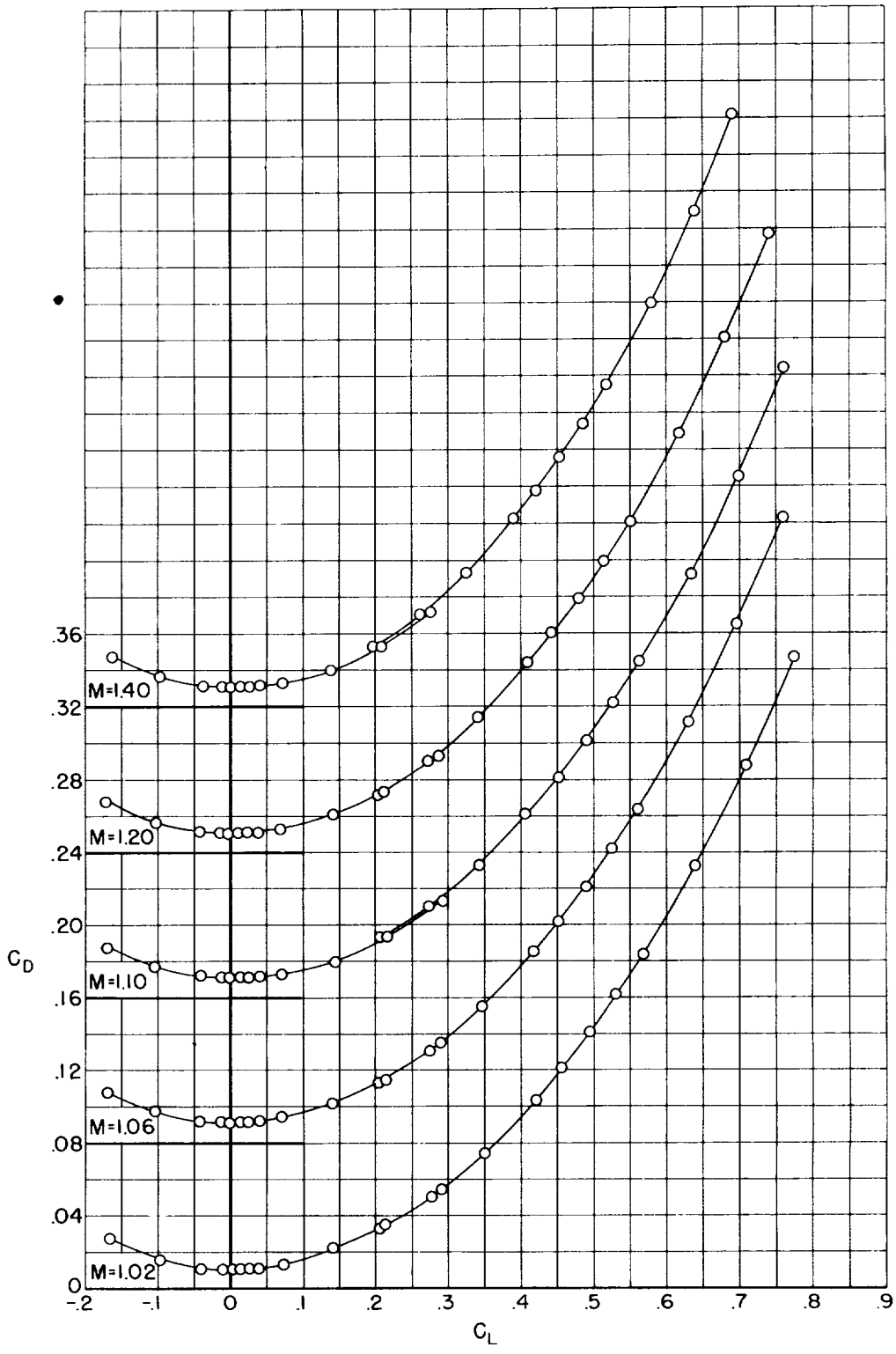

Figure 9.- Forebody drag coefficient for model A.

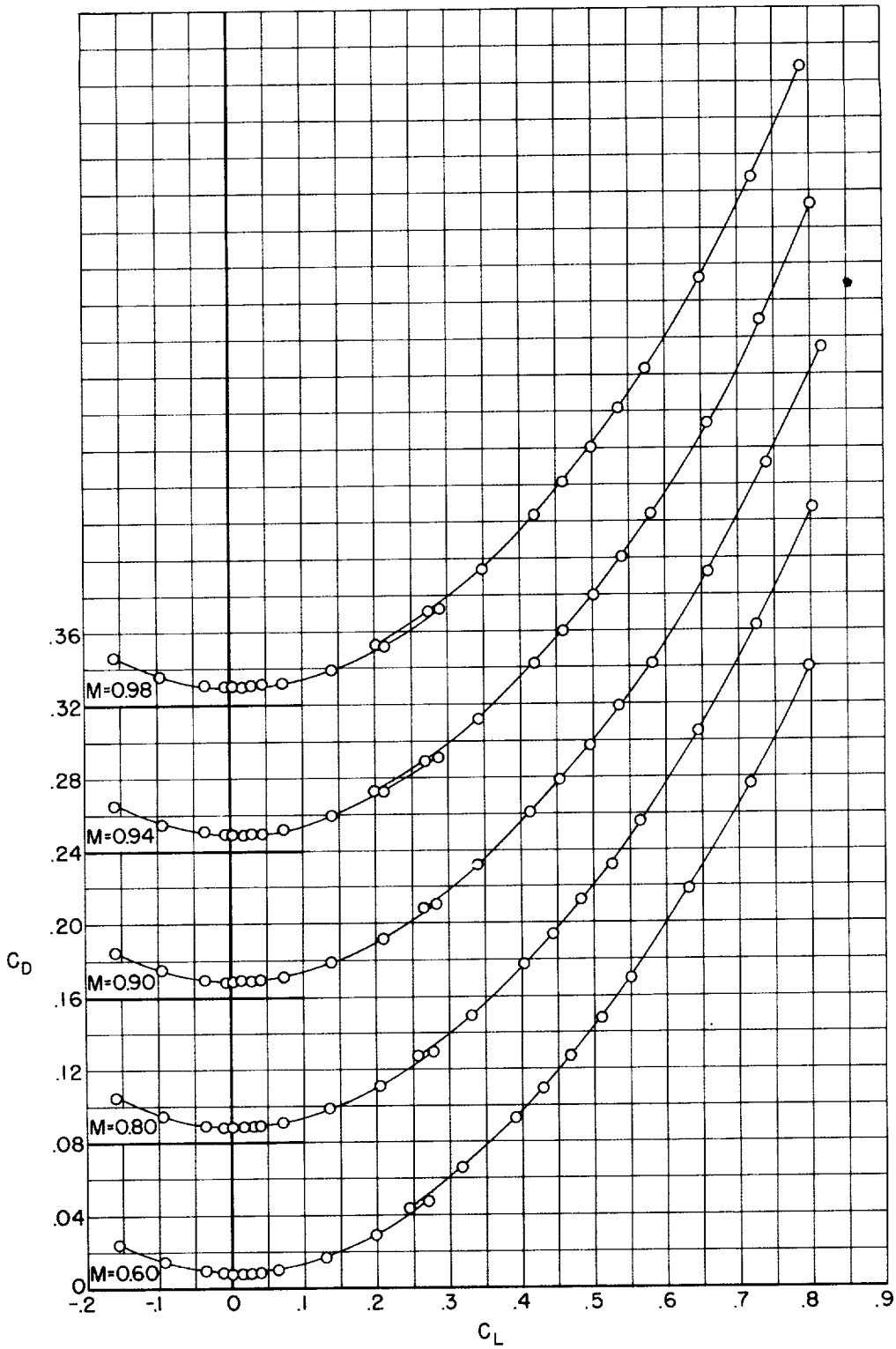

Figure 9.- Concluded.

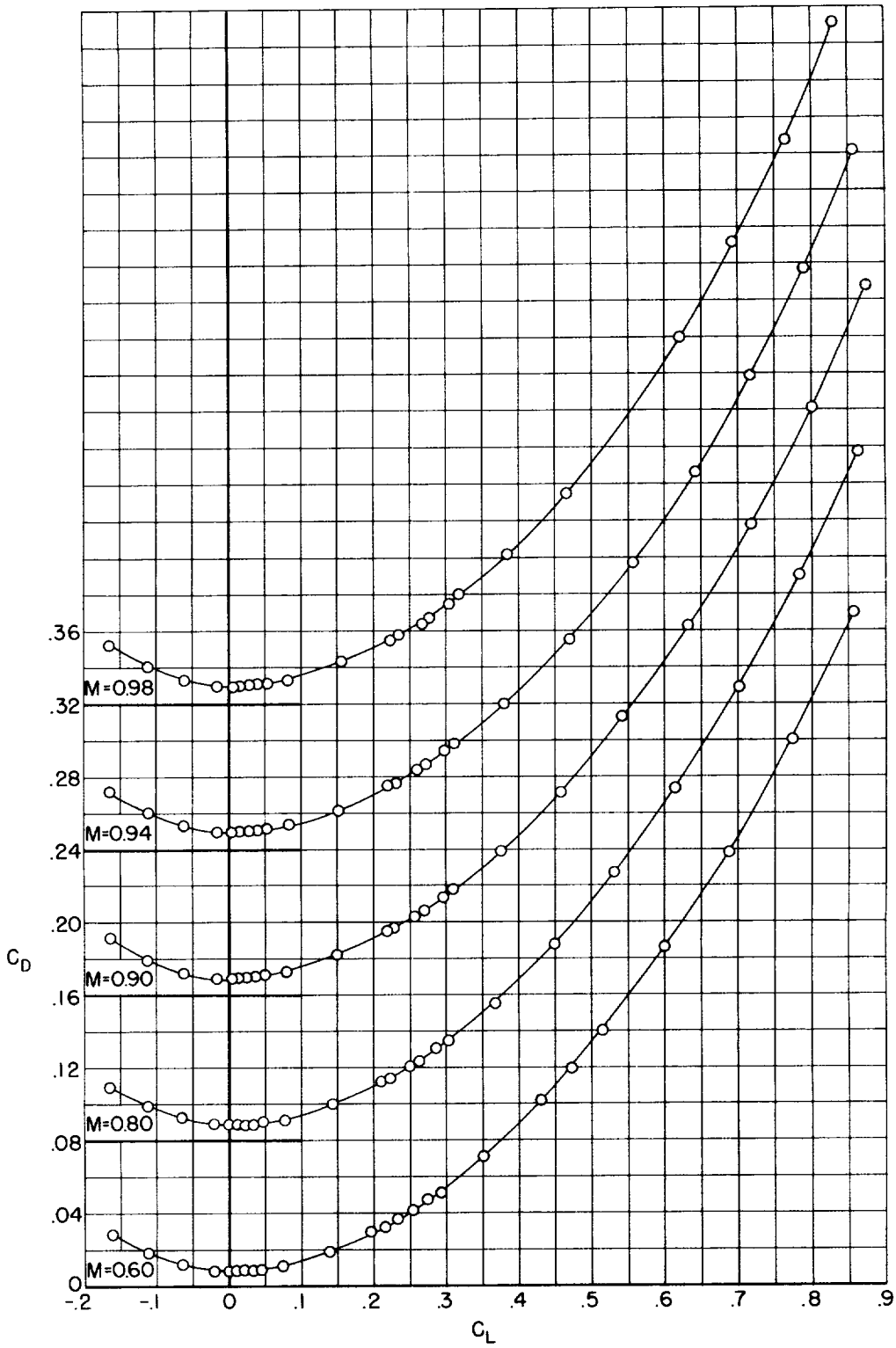

Figure 10.- Forebody drag coefficient for model A_{45}.

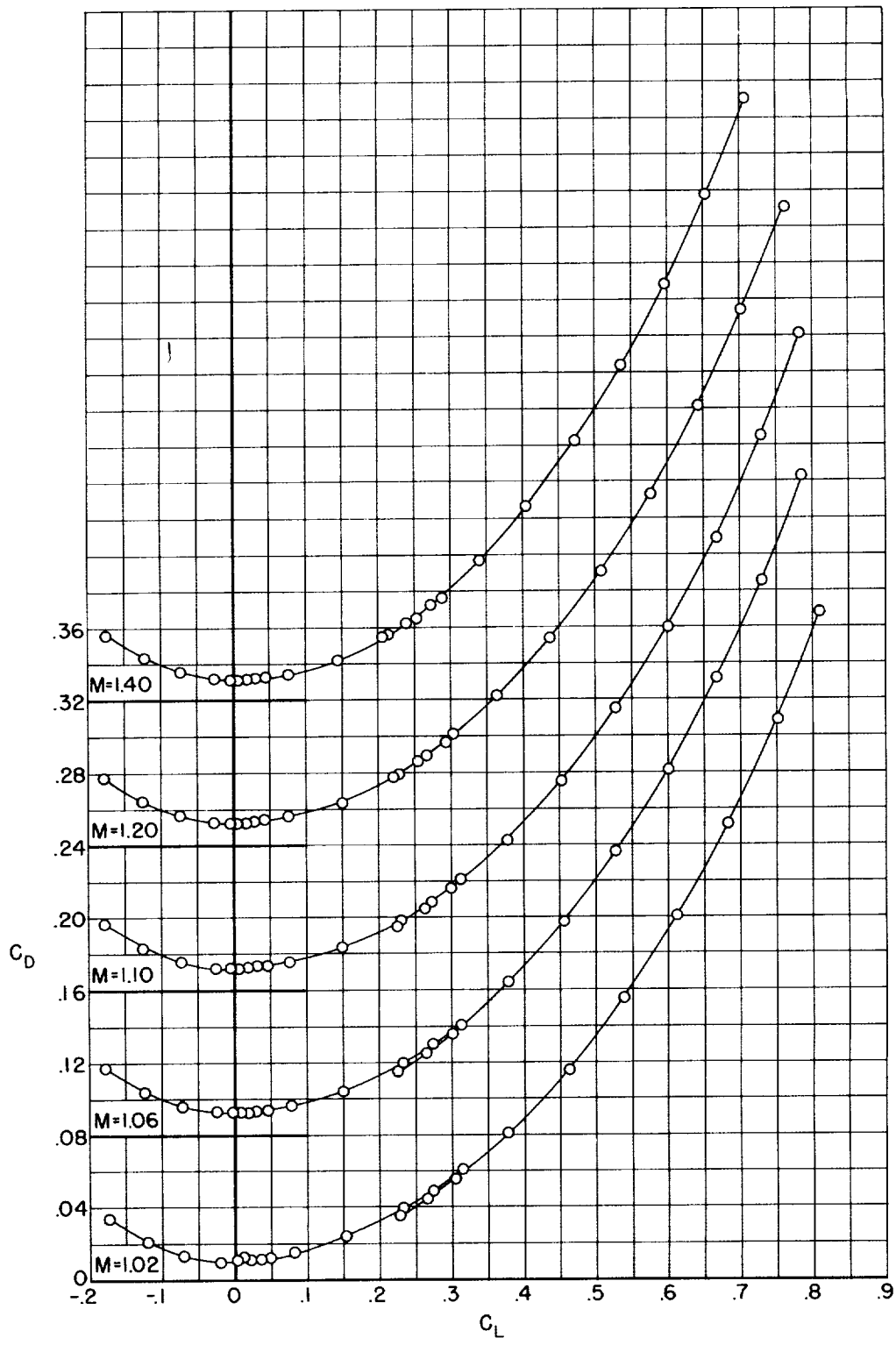

Figure 10.- Concluded.

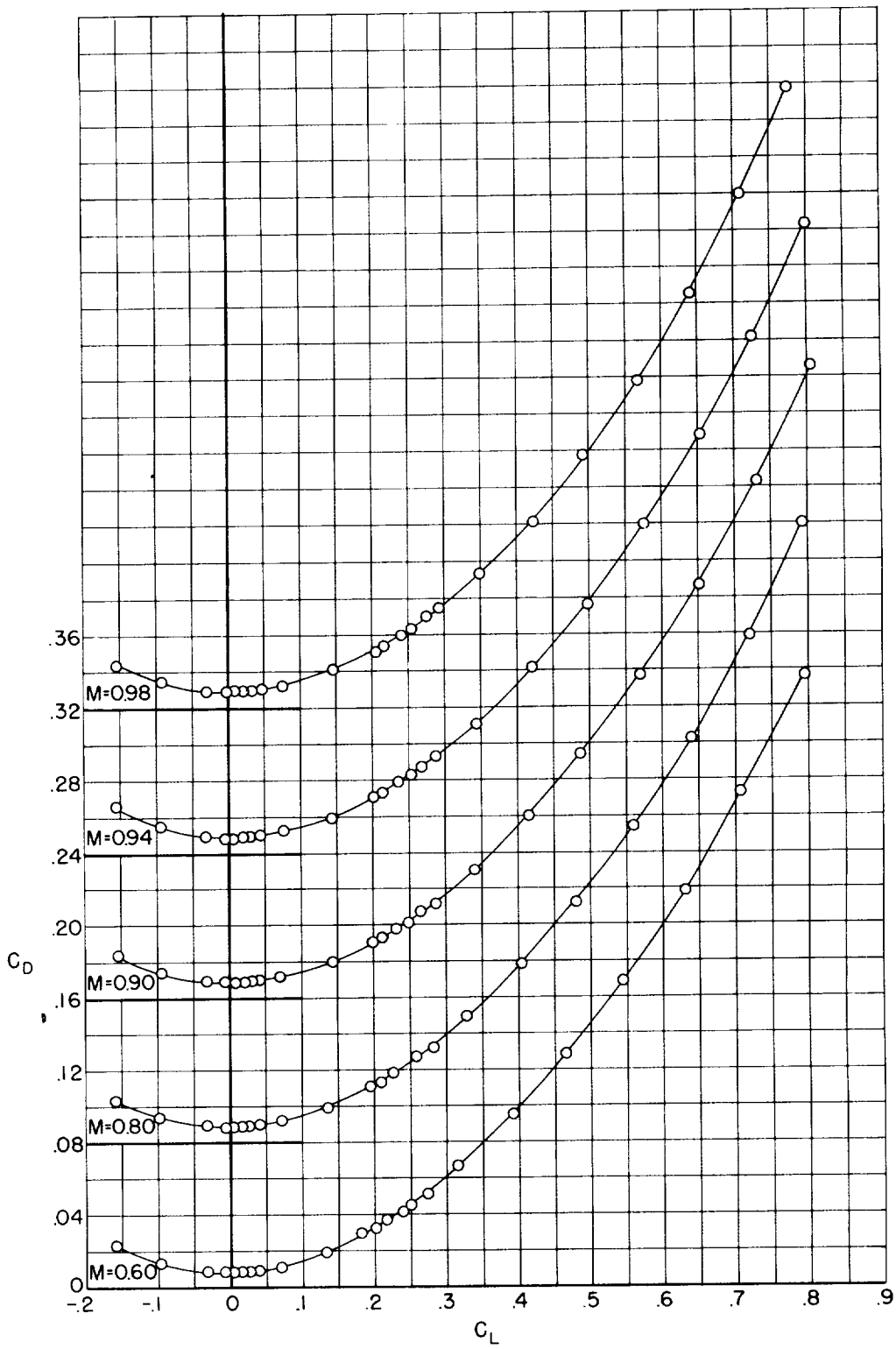

Figure 11.- Forebody drag coefficient for model B.

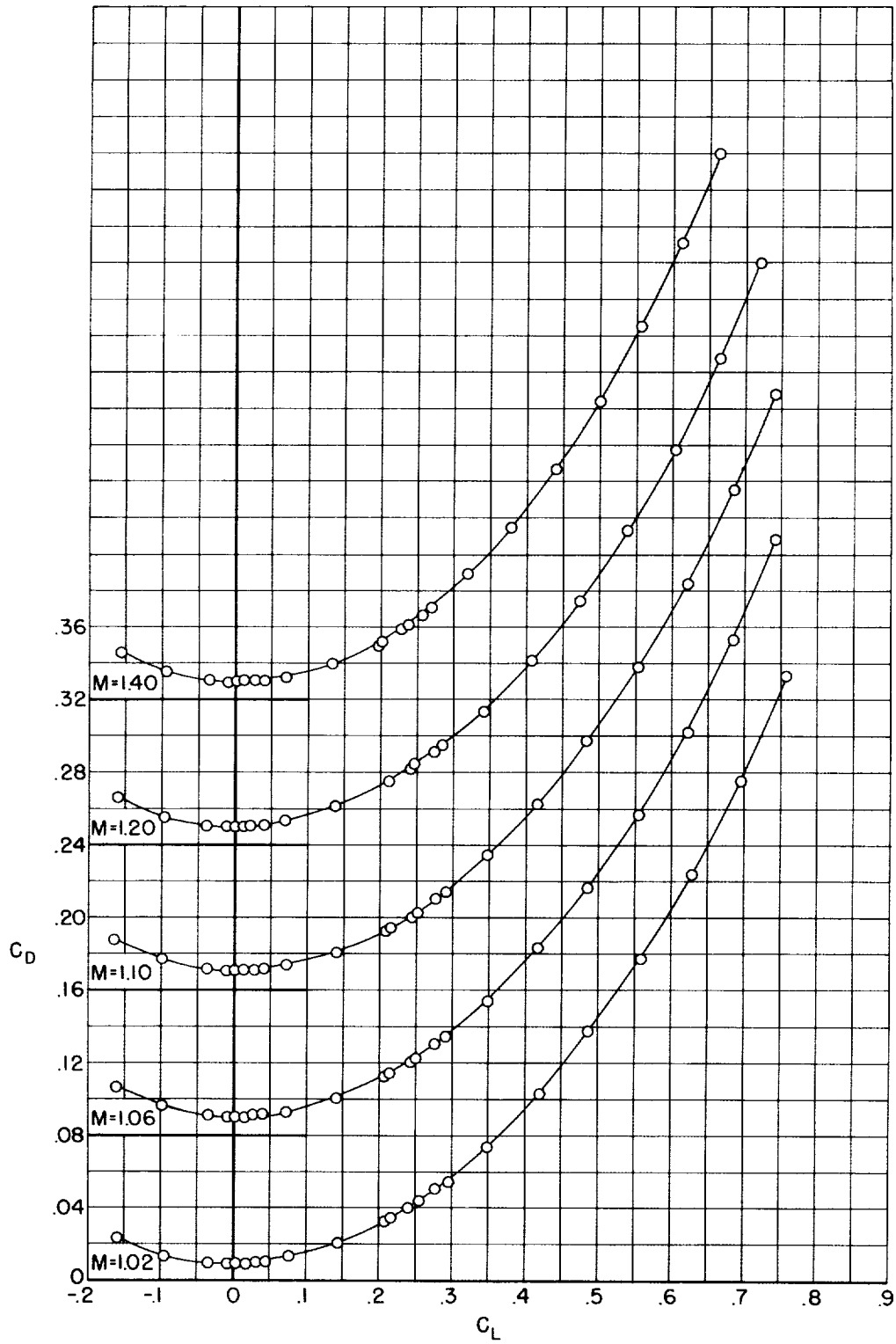

Figure 11.- Concluded.

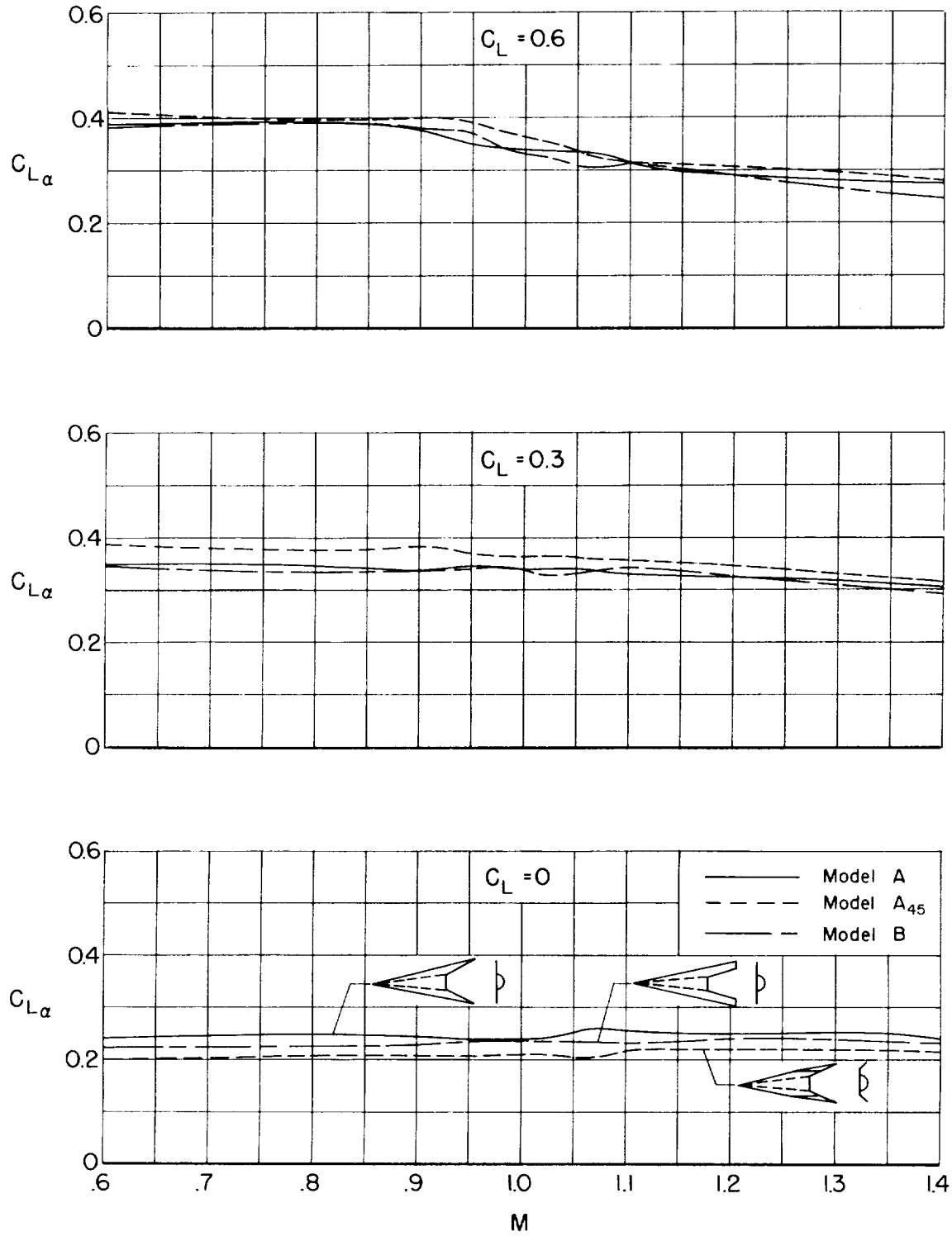

Figure 12.- Effects of wing plan form on lift-curve slope.

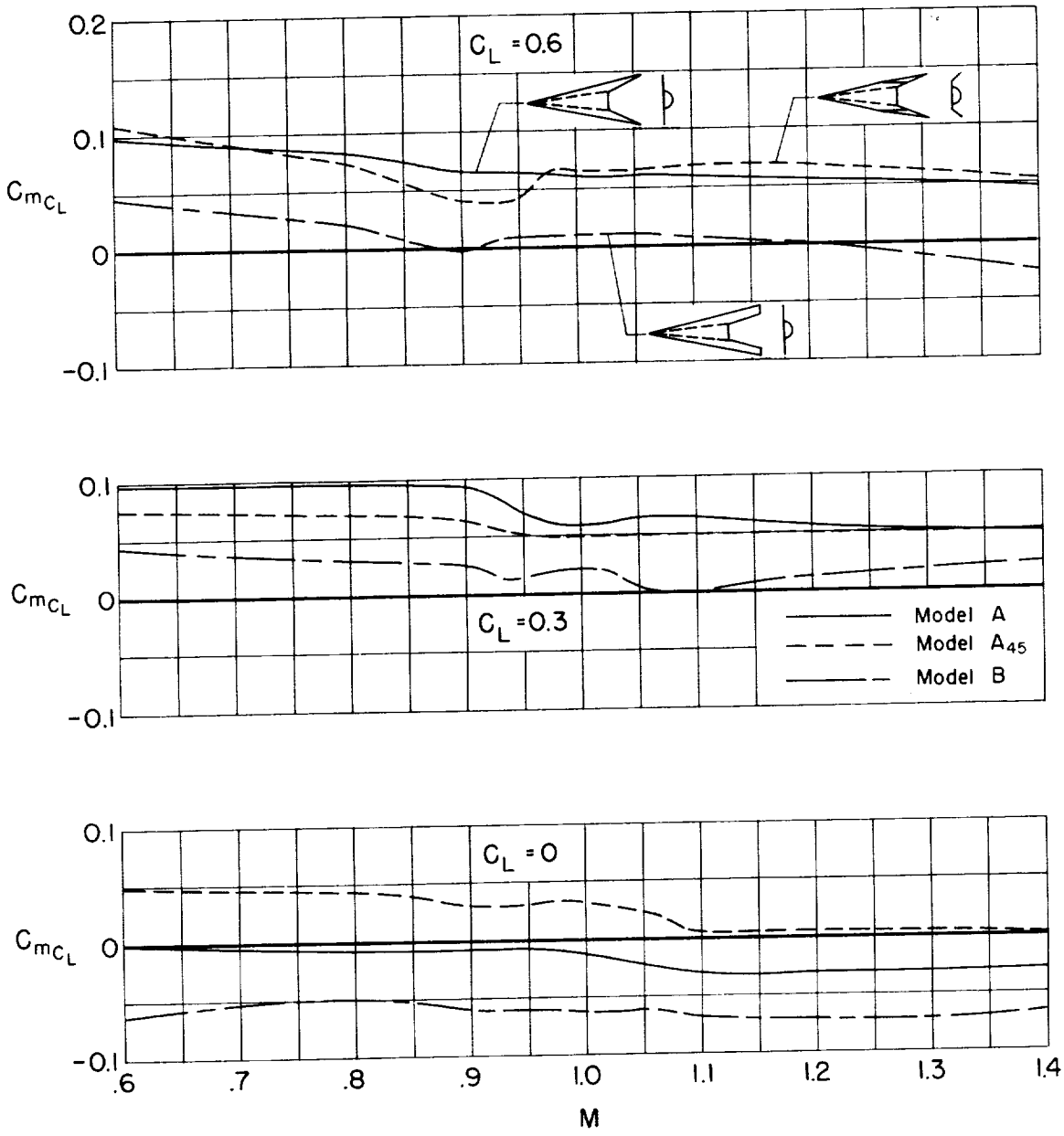

Figure 13.- Effects of wing plan form on pitching-moment-curve slope.

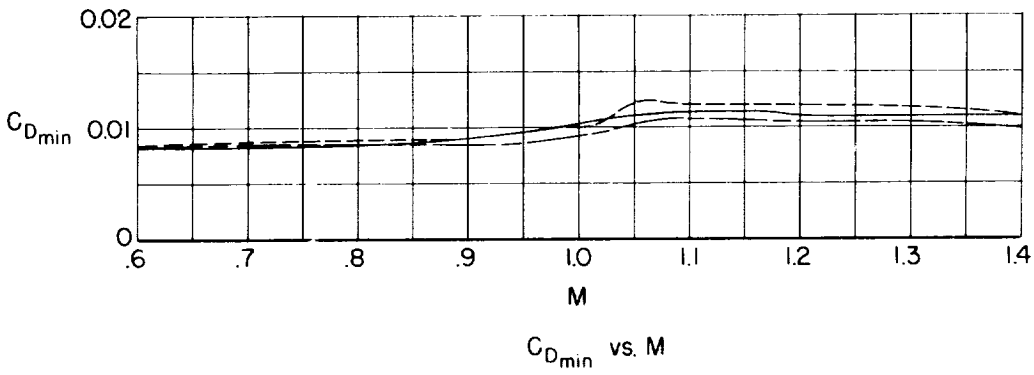

$C_{D_{min}}$ vs. M

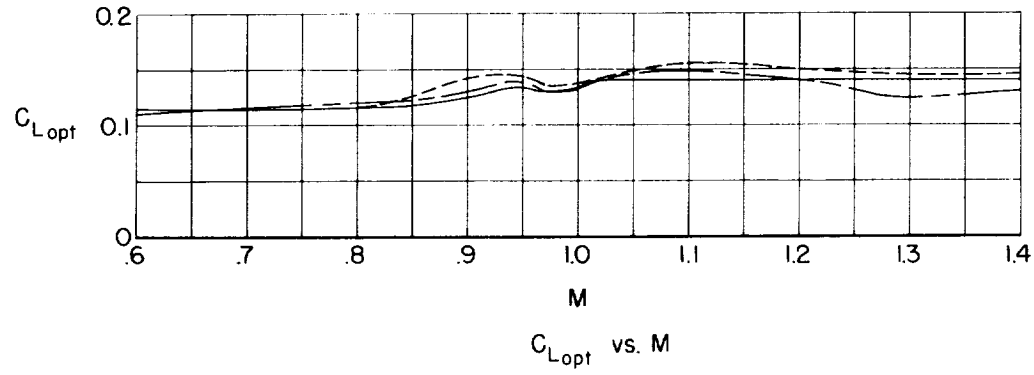

$C_{L_{opt}}$ vs. M

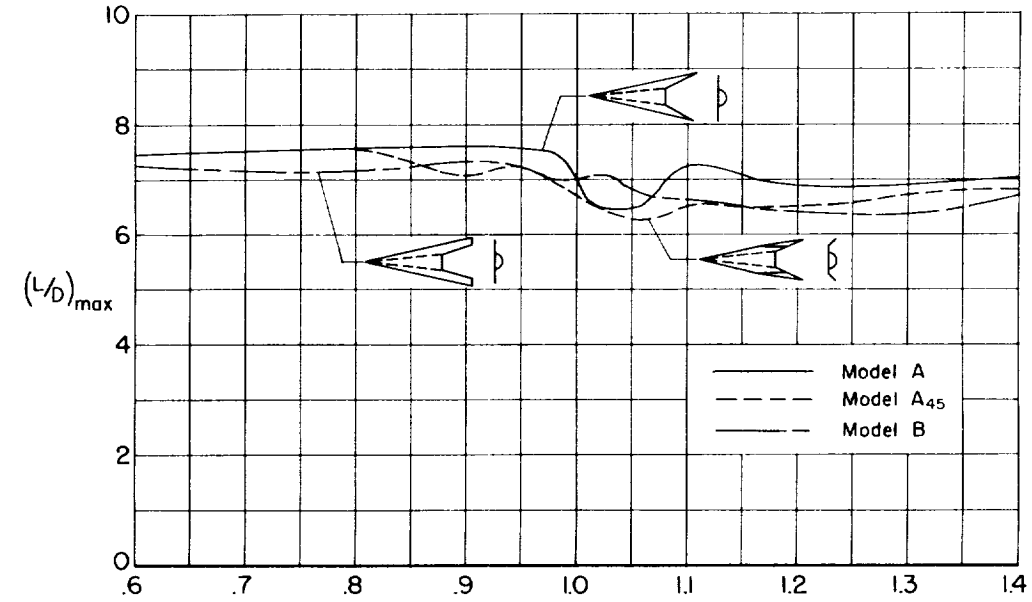

$(L/D)_{max}$ vs. M

Figure 14.- Effects of wing plan form on maximum lift-drag ratio, optimum lift coefficient, and minimum forebody drag coefficient.

NASA - Langley Field, Va. A-237